HIGH-RESOLUTION ESTIMATION OF EVAPOTRANSPIRATION IN NON-IRRIGATED LANDS FOR THE ENTIRE STATE OF NEW MEXICO USING A SOIL WATER BALANCE MODEL – YEAR TWO

By

Jan M.H. Hendrickx
Hydrology Program
Department of Earth & Environmental Science
New Mexico Tech

Peter ReVelle
Hydrology Program
Department of Earth & Environmental Science
New Mexico Tech

David Ketchum
Hydrology Program
Department of Earth & Environmental Science
New Mexico Tech

Daniel Cadol
Hydrology Program
Department of Earth & Environmental Science
New Mexico Tech

FINAL REPORT

Project No. xxxxx

June 2016

New Mexico Water Resources Research Institute.

DISCLAIMER

The New Mexico Water Resources Research Institute and affiliated institutions make no warranties, express or implied, as to the use of the information obtained from this data product. All information included with this product is provided without warranty or any representation of accuracy and timeliness of completeness. Users should be aware that changes may have occurred since this data set was collected and that some parts of these data may no longer represent actual conditions. This information may be updated without notification. Users should not use these data for critical applications without a full awareness of its limitations. This product is for informational purposes only and may not be suitable for legal, engineering, or surveying purposes. The New Mexico Water Resources Research Institute and affiliated institutions shall not be liable for any activity involving these data, installation, fitness of the data for a particular purpose, its use, or analyses results.

ACKNOWLEDGEMENTS

This research was supported by the New Mexico Statewide Water Balance Project, funded through the New Mexico Water Resources Research Institute.

ABSTRACT

Main study objective is the development of a procedure for the calculation of daily reference ETr at a spatial resolution adequate for assessment of evapotranspiration and groundwater recharge in the mountainous regions of New Mexico. The procedure for calculation of the daily ETr over the entire state of New Mexico is described in Chapter 2 and the procedure for calculation of the daily evapotranspiration and groundwater recharge is described in Chapter 3 and with much greater detail in the NMWRRI report by Ketchum et al. [2016]. For the calculation of the reference ETr the topography (slope, azimuth, shading) is taken into account to better assess groundwater recharge in the mountains. Some first results of our algorithms are presented.

Key words: evapotranspiration, reference evapotranspiration, topography, New Mexico

TABLE OF CONTENTS

LIST OF FIGURES

loses 70% of precipitation to evapotranspiration, by far the dominant flux of water from the soil layer [*Ketchum et al.*, 2016].

1. INTRODUCTION

The economic vitality of New Mexico depends on its water availability. However, it is not known exactly where, when and how much water is available in the state. The ongoing statewide integrated water assessment that will consist of the budgets for all major river basins and aquifer systems in the state, addresses this critical information gap for the management of New Mexico's water resources.

Precipitation and evapotranspiration are the major components of the water balance in New Mexico and greatly exceed other components such as runoff, groundwater recharge, and change in soil moisture. Therefore, it is critical to acquire in a cost-effective manner accurate precipitation and evapotranspiration data as input into the statewide water assessment. Since existing meteorological stations in New Mexico don't cover the entire state and leave many areas without accurate information, we have evaluated in Year One the accuracy of existing nationwide operational data bases for precipitation and evapotranspiration for quantification of the spatial and temporal distributions of the precipitation and evapotranspiration components of the state water budget [*Schmugge et al.*, 2016]. We found that the daily PRISM precipitation data base with a spatial resolution of 800 m was adequate for the assessment of statewide precipitation. However, no operational evapotranspiration product was of sufficient quality for statewide evapotranspiration and groundwater recharge assessment. Therefore, in this study we will adapt a proven soil water balance method for the estimation of statewide evapotranspiration for groundwater recharge assessment. This work is complementary to that of other members of the Statewide Water Assessment project who focus on different components of the water balance such as stream flow, groundwater recharge, and changes in aquifer water storage as well as on the statewide energy balance.

Stream flow and groundwater recharge are the drivers for water availability in the state. Because precipitation and evapotranspiration are much larger components of the statewide water budget than stream flow and groundwater recharge combined, a small error in precipitation and/or evapotranspiration will lead to a large error in the estimation of water availability [*Gee and Hillel*, 1988; *Hendrickx and Walker*, 1997; *Kearns and Hendrickx*, 1998]. Accurate evapotranspiration (*ET*) data will greatly improve statewide assessments of the temporal and spatial distributions of groundwater recharge and water availability in New Mexico. ET exceeds precipitation in New Mexico's irrigated and riparian areas and approximately equals it in most rangelands and deserts, but ET is less in mountain recharge areas. As a consequence a small relative error in estimation of precipitation and/or ET in the mountains will often result in a large error of the smaller components of the water balance such as stream flow and groundwater recharge. Therefore, it is critical to acquire accurate, up-to-date, high spatial resolution ET data for input into the statewide water assessment.

The daily latent heat flux λET[1] [MJ m^{-2} day^{-1}] can be calculated directly using the Penman-Monteith equation [Chapter 8 in *Jensen and Allen*, 2016]

$$\lambda ET = \frac{\Delta(R_n - G) + \rho_a c_p \left(\frac{e_s - e_a}{r_a}\right)}{\Delta + \gamma\left(1 + \frac{r_s}{r_a}\right)} \quad (1.1)$$

where λ is the latent heat of vaporization of water [2.45 MJ kg^{-1}], Δ is the slope of saturation vapor pressure vs. temperature [kPa °C^{-1}], ρ_a is mean air density at constant pressure [kg m^{-3}], c_p is the specific heat of water at constant pressure [MJ kg^{-1} °C^{-1}], $(e_s - e_a)$ is the difference between saturated and actual vapor pressure [kPa], r_a and r_s are the bulk aerodynamic and surface resistances [s m^{-1}], R_n is net radiation [MJ m^{-2} day^{-1}], G is the ground heat flux [MJ m^{-2} day^{-1}], and γ is the psychrometric constant [kPa °C^{-1}]. Although examples of this one-step approach for ET calculation have been presented in the literature [e.g., *Beven*, 1979; *Leuning et al.*, 2008] the main difficulty for its operational use is the lack of a data base with effective values for the surface resistance of different crops [*Shuttleworth*, 2006] equivalent to the data bases that exist for the crop coefficient [*Allen et al.*, 1998]. Therefore, rather than a direct ET calculation using Eq. (1.1) the most common application of the Penman-Monteith equation for ET assessment encompasses a two-step process. The first step is the calculation of the reference evapotranspiration for a tall crop ETr and the second step is multiplying ETr by a crop coefficient K_c [*Jensen and Allen*, 2016]

$$ET = K_c \, ET_r \quad (1.2)$$

Generally the K_c has a fixed maximum related to the potential energy available for evapotranspiration which prevents overestimation of *ET*. In addition, the calculation of the reference ETr has been standardized [*Allen et al.*, 1998; *ASCE-EWRI*, 2005; *Smith et al.*, 1991] so that ET values calculated for different locations and dates can be compared to each other.

Application of Eq. (1.2) is straightforward on flat irrigated and riparian lands with full water availability but its use in flat areas with limited water availability requires the implementation of a daily soil water balance model to account for the effects of decreasing available water on ET [e.g. *Allen et al.*, 1998; *Jensen and Allen*, 2015; *Ritchie*, 1972]. Such a model will not only yield a robust estimate of ET but also of groundwater recharge [*Daniel B. Stephens & Associates*, 2010; *Sandia National Laboratory*, 2007] while respecting closure of the water and energy balances. In mountainous areas an additional step is required: the reference ETr

[1] For water with a density of 1,000 kg/m^3 and at a temperature of 20 °C the ET in mm/day equals $\lambda ET/2.45 = 0.408 \lambda ET$.

needs to be adjusted for each pixel of the daily soil water balance model to take into account the effects of slope, azimuth and elevation on incoming solar radiation [e.g., *Aguilar et al.*, 2010].

To fill the lack of operational ET and groundwater recharge products that cover the entire state of New Mexico, we developed a simple Evapotranspiration and Recharge Model (ETRM) that accounts for all water inputs and outputs on a daily basis over the entire area of the state at a spatial resolution of 250 m. Water partitioned to *ET*, groundwater recharge, and runoff balances the input from precipitation and storage in the soil layer [*Ketchum et al.*, 2016]. The initial results of ETRM in 2015 revealed that its calculations of *ET* were adequate in relatively flat lower-elevation areas. The ETRM results of 2015, however, failed in high-elevation mountainous areas. This was mainly due to the coarse spatial scale of about 12×12 km for the reference ETr obtained from *Lewis et al.* [2014] that neglects the effects of elevation and topography on *ET*. For example, no distinction was made between north and south facing slopes, or between a flat pixel and one in the bottom of a narrow canyon without direct exposure to sunlight. Yet, in southern Spain at the same latitude as northern New Mexico *Aguilar et al.* [2010] found that the use of topography-adjusted incoming solar radiation for calculation of the reference ETr is of critical hydrologic importance. Therefore, the main objective of this study is to develop a procedure for the calculation of daily ETr at a spatial resolution adequate for assessment of evapotranspiration and groundwater recharge in the mountainous regions of New Mexico.

2. CALCULATION OF TOPOGRAPHY-ADJUSTED REFERENCE ETr

The calculation of the reference *ET* is straightforward in flat irrigated lands where high quality meteorological data are available. Under these conditions the reference *ET* can be calculated using the standardized reference evapotranspiration equations of the *ASCE-EWRI* [2005]. Two reference *ET* equations are available: the *ETo* equation for a short crop (clipped grass with approximate height of 0.12 m) and the ETr equation for a tall crop (full-cover alfalfa with approximate height 0.50 m). Each reference crop has its unique advantages for specific land covers and periods of the year. Each reference also has its own unique set of crop coefficients. One cannot use the crop coefficients for ETo in the ETr equation and vice versa. For the statewide water assessment the reference ETr for a tall crop is used because it is more representative of the surface roughness of native vegetation in New Mexico than the reference ETo for a short crop.

The daily reference ETr is defined as the daily *ET* from "a hypothetical extensive surface of a [alfalfa] crop that is well-watered, and fully shades the ground with an assumed crop height of 0.50 m, a fixed surface resistance r_s of 45 s m^{-1} and an albedo of 0.23" [*ASCE-EWRI*, 2005]. This ETr is calculated using Eq. (1.1) after dividing its right-hand side by the latent heat of vaporization of water (λ) and putting the daily soil heat flux (G) equal to zero

$$ETr_{daily} = 0.408\ \frac{\Delta\, R_n + \rho_a c_p \left(\frac{e_s - e_a}{r_a}\right)}{\Delta + \gamma\left(1 + \frac{r_s}{r_a}\right)} \tag{2.1}$$

where ETr has units of mm/day and the constant 0.408 equals 1/λ.

2.1 Calculation of the Daily Reference ETr in Flat Lands

The calculations of ETr_{daily} start with the calculation of the daily mean air temperature T [°C] as

$$T = \frac{T_{max} + T_{min}}{2} \tag{2.2}$$

where T_{max} and T_{min} are the daily maximum and minimum air temperature [°C]. Next, the mean atmospheric pressure P [kPa] at the weather station (or pixel of interest) is predicted with a simplified version of the universal gas law as

$$P = 101.3\ \left(\frac{293 - 0.0065\, z}{293}\right)^{5.26} \tag{2.3}$$

where z is the site elevation above sea level [m] and the ambient temperature is 20 °C. The psychometric constant γ [kPa °C^{-1}] is proportional to the mean atmospheric pressure as

$$\gamma = 0.000665\ P \tag{2.4}$$

The slope of the saturation vapor pressure-temperature curve Δ [kPa °C^{-1}] is calculated as

$$\Delta = \frac{2504\ exp\left(\frac{17.27\ T}{T+237.3}\right)}{(T+237.3)^2} \tag{2.5}$$

The saturated vapor pressure e_s (kPa) is a measure of the maximum amount of water vapor that the air can hold

$$e_s = \frac{e^o(T_{max})+e^o(T_{min})}{2} \tag{2.6}$$

where $e^o(T)$ is the saturation vapor pressure function

$$e^o(T) = 0.6108\ exp\left(\frac{17.27\ T}{T+237.3}\right) \tag{2.7}$$

with temperature in °C.

The actual vapor pressure e_a (kPa) represents the water content or humidity of the air and can be measured or calculated from various humidity data including dew point temperature or relative humidity and air temperature data [e.g., *ASCE-EWRI*, 2005]. In this study the actual vapor pressure is calculated from the specific humidity q [kg kg^{-1}] as

$$q = \frac{m_v}{m_v+m_d} = \frac{w}{1+w} \tag{2.8}$$

where m_v is the mass of water vapor in a unit mass of air (mass of dry air m_d plus mass of water vapor m_v) and w is the ratio of the mass of water m_v to the mass of dry air m_d

$$w = \frac{m_v}{m_d} \tag{2.9}$$

Both q and w are often expressed in grams of water vapor per kilogram of, respectively, moist and dry air but in calculations they should be expressed as *dimensionless* numbers, e.g., as kg of water per kg of moist or dry air [*Wallace and Hobbs*, 2006]. The specific humidity q is related to the actual vapor pressure e_a as [*Monteith and Unsworth*, 2008]

$$e_a = \frac{q\ P}{0.622 + 0.378\ q} \approx \frac{q\ P}{0.622} \tag{2.10}$$

The dew point temperature T_{dew} can be calculated from e_a as [*Allen et al.*, 1998]

$$T_{dew} = \frac{116.91+237.3\ \ln(e_a)}{16.78-\ln(e_a)} \tag{2.11}$$

The relative humidity RH [%] is calculated as

$$RH = \frac{e_a}{e_s}\ 100 \tag{2.12}$$

The net radiation R_n is the energy available at the land surface for evaporating and transpiring water and heating the air; it is the sum of the net short wave R_{ns} and long wave R_{nl} radiation

$$R_n = R_{ns} - R_{nl} \tag{2.13}$$

where R_{ns} is defined as being positive downwards and negative upwards and R_{nl} being positive upwards and negative downwards. Both net radiation components generally have positive or zero values.

The net solar or short-wave radiation is

$$R_{ns} = R_s - \alpha R_s = (1 - \alpha) R_s \tag{2.14}$$

where R_s is the incoming solar radiation [MJ m^{-2} d^{-1}] and α the albedo or canopy reflection coefficient [-] that is fixed at 0.23 for the standardized tall reference surface.

The net long-wave radiation for a moist reference surface only can be calculated as

$$R_{nl} = \sigma \left[\frac{T_{K\,max}^4 + T_{K\,min}^4}{2}\right] (0.34 - 0.14\sqrt{e_a}) \left(1.35 \frac{R_s}{R_{so}} - 0.35\right) \tag{2.15}$$

where σ is the Stefan-Boltzmann constant [4.901×10^{-9} MJ K^{-4} m^{-2} d^{-1}], $T_{K\,max}$ is the maximum absolute temperature during the 24-hour period [K] (K = °C + 273.16), $T_{K\,min}$ is the minimum absolute temperature during the 24-hour period [K] (K = °C + 273.16), R_s/R_{so} is the relative solar radiation, R_s is the measured or calculated solar radiation and R_{so} is the calculated clear-sky radiation. The ratio R_s/R_{so} is an indication of the relative cloudiness and its value must be limited to $0.25 < R_s/R_{so} \leq 1.0$).

An approximation for the clear-sky radiation R_{so} to be used in Eq. (2.15) is

$$R_{so} = (0.75 + 2 \times 10^{-5} z)\, R_a \tag{2.16}$$

where z is the elevation above sea level [m] and R_a is the extraterrestrial radiation [MJ m^{-2} d^{-1}]. Eq. (2.16) was used in this study due to memory issues while calculating statewide daily R_{so} values for each pixel. For future applications a more accurate procedure will be used that considers the effects of sun angle and water vapor on absorption of short wave radiation and separates the components of beam and diffuse radiation

$$R_{so} = (K_B + K_D) R_a \tag{2.17}$$

where K_B is the clearness index for direct beam radiation [-], K_D is the clearness index for diffuse radiation [-] and R_a is the extraterrestrial radiation [MJ m^{-2} d^{-1}].

$$K_B = 0.98\, exp\left[\frac{-0.00146\, P}{K_{turb}\, sin\phi} - 0.075 \left(\frac{W}{sin\phi}\right)^{0.4}\right] \tag{2.18}$$

where K_{turb} is a turbidity coefficient [-] $0 < K_{turb} \leq 1.0$ with $K_{turb} = 1.0$ for clean air and $K_{turb} \leq 0.5$ for extremely turbid, dusty or polluted air; P is atmospheric pressure calculated with Eq. (2.3), f is the angle of the sun above the horizon [radians] and W is precipitable water in the atmosphere [mm]. In this study we use $K_{turb} = 1.0$.

For daily (24-hour) time periods the average value of f weighted according to R_a can be approximated as

$$sin\phi_{24} = sin\left[0.85 + 0.3\,\varphi\, sin\left(\frac{2\,\pi}{365}J - 1.39\right) - 0.42\,\phi^2\right] \tag{2.19}$$

where f_{24} is the average f during the daylight period, weighted according to R_a, φ is the latitude [radians] and J is the Julian day [-]. The "$sin\phi_{24}$" variable should be used in Eq. (2.18) instead of $sin\phi$ and its value should be limited to greater than or equal to 0.

Precipitable water W is predicted as

$$W = 0.14\, e_a\, P + 2.1 \tag{2.20}$$

and the diffuse radiation index K_D is estimated from K_B as

$$K_D = 0.35 - 0.36\, K_B \tag{2.21}$$

The daily extraterrestrial radiation R_a [MJ m^{-2} d^{-1}] is estimated as

$$R_a = \frac{24}{\pi}\, G_{sc}\, d_r\, [\omega_s \sin(\varphi) \sin(\delta) + \cos(\varphi) \cos(\delta) \sin(\omega_s)] \tag{2.22}$$

where G_{sc} is the solar constant [4.92 MJ m^{-2} d^{-1}], d_r is the inverse relative distance factor (squared) for the earth-sun [-], v_s is the sunset hour angle [radians] and d is the solar declination [radians]. The last three variables are calculated as

$$d_r = 1 + 0.033\, cos\left(\frac{2\pi}{365}J\right) \tag{2.23}$$

$$\omega_s = \arccos[-\tan(\varphi)\tan(\delta)] \tag{2.24}$$

$$\delta = 0.409\, sin\left(\frac{2\pi}{365}J - 1.39\right) \tag{2.25}$$

The aerodynamic resistance r_a between the surface and height z for use in Eq. (2.1) is calculated as

$$r_a = \frac{\left[ln\left(\frac{z_u - d}{z_{om}}\right) - \Psi_m\right]\left[ln\left(\frac{z_{T,e} - d}{z_{oh}}\right) - \Psi_h\right]}{k^2\, u_z} \tag{2.26}$$

where k is the von Kármán constant [0.41], z_u is measurement height for wind speed u, $z_{T,\,e}$ is measurement height for temperature and vapor pressure, u_z is the windspeed u at height z, d is the displacement height [m], z_{om} is the roughness length for momentum transport, z_{oh} is the roughness length for heat and vapor transport, Ψ_m and Ψ_h are dimensionless stability parameters that can be set equal to zero for moist reference surfaces where near-neutral stability conditions exist.

Finally, after standardization the daily reference ETr for flat terrain becomes [Chapter 8 in *Jensen and Allen*, 2016]

$$ETr_{daily} = \frac{0.408\,\Delta\,R_n + \gamma\frac{1600}{T+273}u_2\,(e_s - e_a)}{\Delta + \gamma(1+0.38\,u_2)} \qquad (2.27)$$

2.2 Calculation of the Daily Reference ETr in Mountains

The study of weather in the mountains is very different than in flat regions [*Barry*, 2008]. First, physical access to mountain sites is often difficult which makes the installation and maintenance of weather stations challenging. Second, the spatial variability of mountain terrain topography results in a wide range of weather conditions over short distances so that any weather station can only be representative of a limited area. Third, even standard weather observations in mountains are often difficult due to strong winds and a high proportion of precipitation occurring as snow that is difficult to measure [e.g., *Nitu and Wong*, 2010]. In addition, local topography may cause observations to be unrepresentative for certain wind directions [*Barry*, 2008]. For these reasons it will not be possible to base the modeling of reference ETr only on meteorological measurements from weather stations as is common in flat populated regions. Instead for this study gridded weather data from the North American Land Data Assimilation System (NLDAS) [*Cosgrove et al.*, 2003] is used as the principal source of meteorological input data. Selected quality controlled meteorological measurements are used for validation purposes. *Senay et al.* [2008] evaluated the use of the Global Data Assimilation System (GDAS) of the National Oceanic and Atmospheric Administration (NOAA) for the worldwide calculation of the daily reference *ETo* at 1-degree spatial resolution. They made daily reference ETo estimates at different spatial and temporal scales for the period 2002 – 2006. Despite the large difference in spatial scale (point *vs*. ~100 km grid cell) between the two data sets, a comparison against daily reference ETo estimates from 85 weather station in California yielded correlations between weather station ETo and GDAS-*ETo* exceeding 0.97 on a daily basis to more than 0.99 on time scales of more than 10 days. Nevertheless, *Senay et al.* [2008] also found that site-specific use of GDAS ETo in "rugged terrain" requires bias correction and/or disaggregation of the GDAS values using downscaling techniques. The mountainous regions of New Mexico certainly fall in this category and reliable

daily reference ETr values can only be obtained by disaggregation of the large km-size cells of the national NLDAS and global GDAS data bases.

The pixel size of the Evapotranspiration and Recharge Model (ETRM) is 250×250 m because (1) this size matches the MOD13Q1 Normalized Difference Vegetation Index (NDVI) product that is used for calculation of the crop coefficient for each pixel using Eq. (3.2); and (2) our current computer facilities can make all necessary computations statewide within a reasonable amount of time. In the future, the spatial resolution can be improved from 250 to 30 m to better capture recharge hot spots in the mountains. Input data for the calculation of the daily topography-adjusted ETr for the period 2000 – 2013 are: 30 m DEM that was aggregated and resampled to 250 m, incoming hourly global horizontal radiation R_g from NLDAS 1/8° (~12.5×12.5 km), daily meteorological data from UofI METDATA 1/24° (~4.0×4.0 km): minimum and maximum air temperature (T_{min}, T_{max}) [°C], specific humidity (q) [kg kg^{-1}] and average wind speed at a height of 10 m (u_{10}) [m s^{-1}].

2.2.1 Disaggregation of Global Radiation

Global radiation is the total amount of solar radiation received by a horizontal surface on the land surface. When solar radiation enters the earth's atmosphere its quantity, quality and direction are noticeably modified by atmospheric scattering and adsorption [e.g., *Monteith and Unsworth*, 2008]. The quantity of radiation refers to its total energy while the quality refers to the distribution of that energy over different wave lengths. The intensity of atmospheric attenuation depends on the path length of the solar beam as well as the amount of attenuating constituents in the path. The path length is often expressed as the *air mass number m* that is equal to the length of the path relative to the depth of the atmosphere. Water vapor is the most variable absorbing gas in the atmosphere and its effect on absorption is quantified by the depth of precipitable water that can be estimated with Eq. (2.20).

As a result of atmospheric attenuation solar radiation has two distinct directional properties when it reaches the land surface. The *direct* or *beam* radiation originates directly from the solar disc and includes a small amount of directly forward scattered radiation. The *diffuse* radiation includes all other scattered radiation received from the blue sky and from clouds, either by reflection or by transmission. *Total* or *global* radiation received on a horizontal land surface consists of the sum of the direct and diffuse radiation. It is the global radiation R_h on a horizontal surface that is typically measured at weather stations and presented by data bases such as NLDAS and METDATA. For a horizontal surface, data of the global incoming solar radiation suffice for calculation of the reference ETr but for inclined surfaces the incoming solar radiation R_s can only be calculated after disaggregation of the global radiation into its direct and diffuse components. Once the direct or beam radiation R_b and diffuse radiation R_d on a horizontal surface are known the total irradiance on an inclined surface R_g is the sum of the beam flux density plus

the diffuse flux density plus an additional flux density of solar radiation reflected from the surfaces surrounding the inclined surface under consideration:

$$R_g = R_{bn}\, cos\theta + C_{top}\, R_d + R_r \tag{2.28}$$

where R_g is the topography-adjusted incoming global radiation on an inclined surface, R_{bn} is the incoming beam radiation on a surface perpendicular to the solar rays, θ is the incidence angle (i.e., the angle between the sun direction and the normal to the inclined surface), C_{top} is a conversion coefficient taking into account the sky view factor and the horizon angle, R_d is the diffuse radiation on a horizontal surface, and R_r is the solar radiation reflected from surrounding surfaces.

When R_h has been measured or estimated at an elevation z that is different from the elevation of the pixel under consideration, an "elevation" or "optical path length" correction must be applied before proceeding to Eq. (2.28). In this study the NLDAS R_h based on a DEM with spatial resolution 12.5 km must be downscaled to the ETRM spatial resolution of 250 m before reference ETr can be calculated. Not only R_h needs to be corrected for elevation but also P, T_{min} and T_{max}, and q. In this study, first R_g is calculated for each hour and summed to the daily R_{g24} (Fig. 2.1). Next, the daily P, T_{min} and T_{max}, q and u_2 are calculated followed by the calculation of the daily ET_r (Fig. 2.2).

2.2.1.1 Elevation and Optical Path Adjustment

The R_h that is representative for a NLDAS pixel (12.5 km) at a fixed elevation needs to be adjusted to become representative for the elevations of the 2500 DEM pixels (250 m) located within this NLDAS pixel. Global radiation that passes through the atmosphere is gradually decreased due to the relative length of air mass m [fraction] it has to pass through and the transmissivity of the sky τ [fraction]. Most of this decrease is caused by a decrease in beam radiation. For example, Fig. 2.3 shows the change of global irradiance and its components (beam irradiance and diffuse irradiance) as a function of altitude. Although the diffuse irradiance decreases by about 50 Wm^{-2} between sea level and an altitude of 5000 m, the beam irradiance drives the change in global irradiance by increasing about 450 Wm^{-2}. Therefore, the elevation adjustment is only made in NLDAS grid cells that represent cloudless conditions under which this adjustment is straightforward. The criterion for cloudless conditions is that the air-mass corrected clearness index K_t' [*Perez et al.*, 1990] exceeds 0.65. Typically, the clearness index K_t is defined on a daily or hourly basis as

$$K_t = \frac{R_{sh}}{R_{ah}} \tag{2.29}$$

where R_{sh} is the measured or calculated hourly solar or global radiation [MJ m^{-2} $hour^{-1}$] and R_{ah} [MJ m^{-2} $hour^{-1}$] is the hourly extraterrestrial radiation

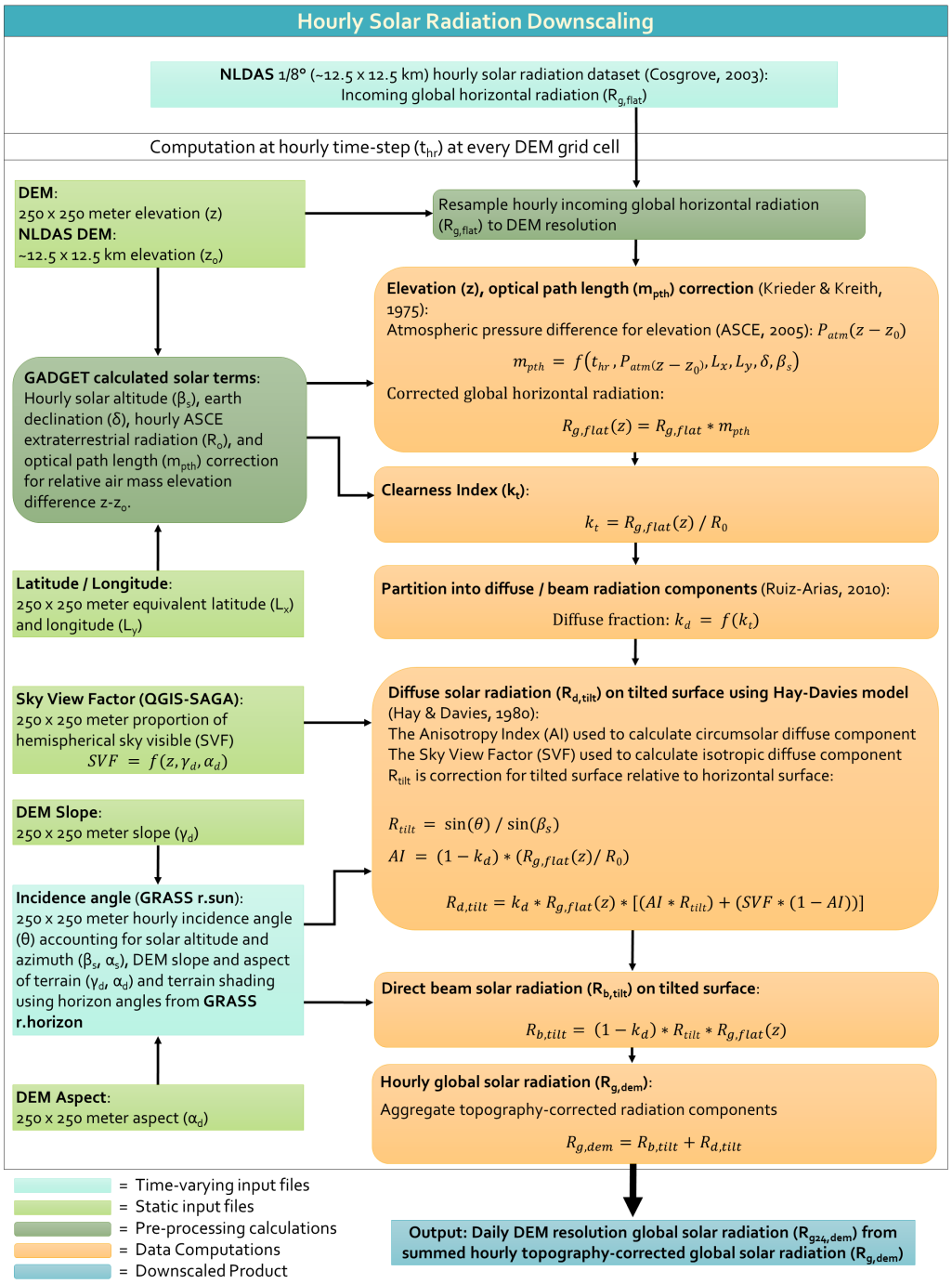

Figure 2.1 Schematic for the calculation of the daily global solar radiation adjusted for topography with a spatial resolution of 250 m.

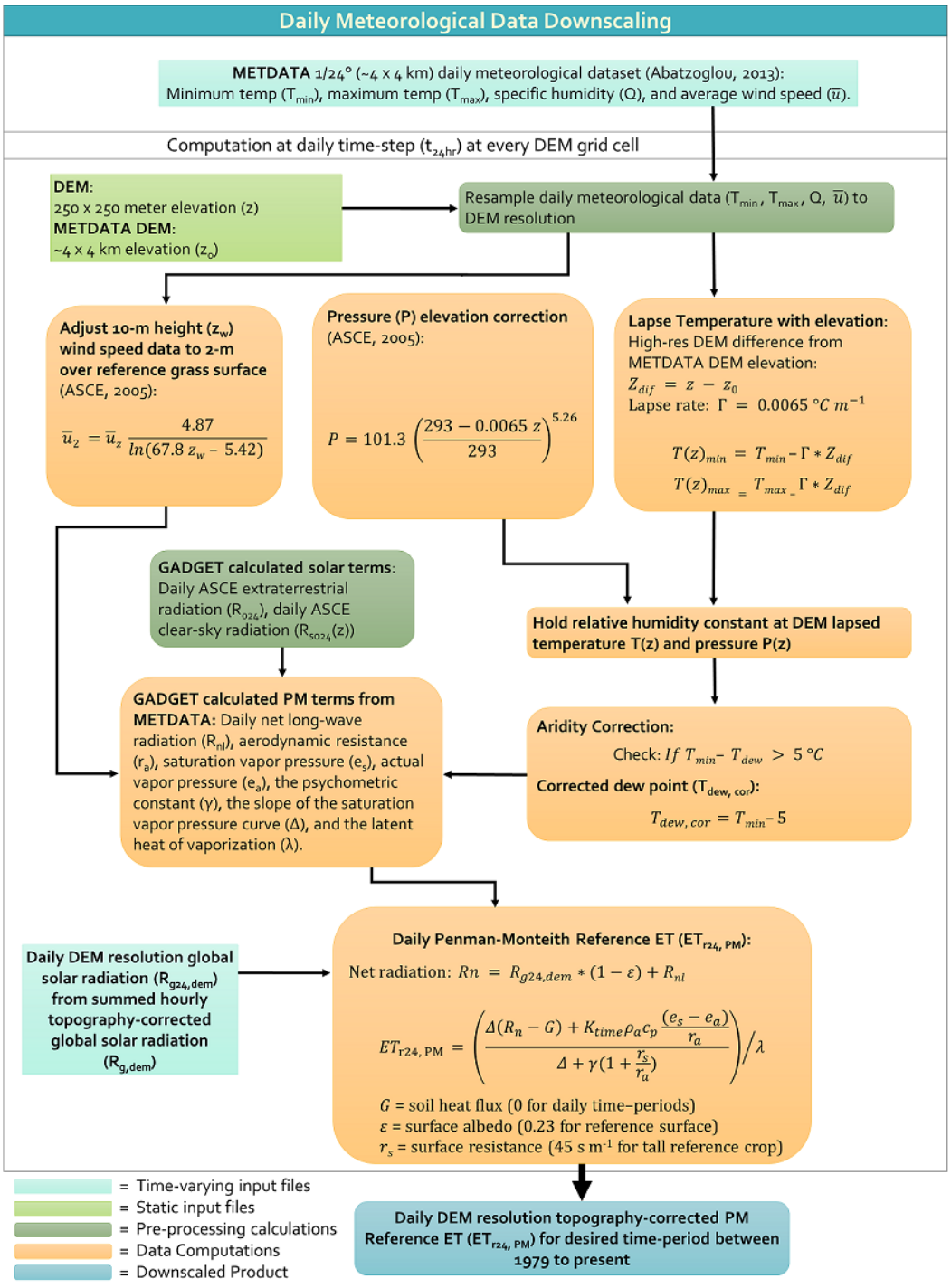

Figure 2.2 Schematic for the calculation of the daily reference ETr adjusted for topography with a spatial resolution of 250 m.

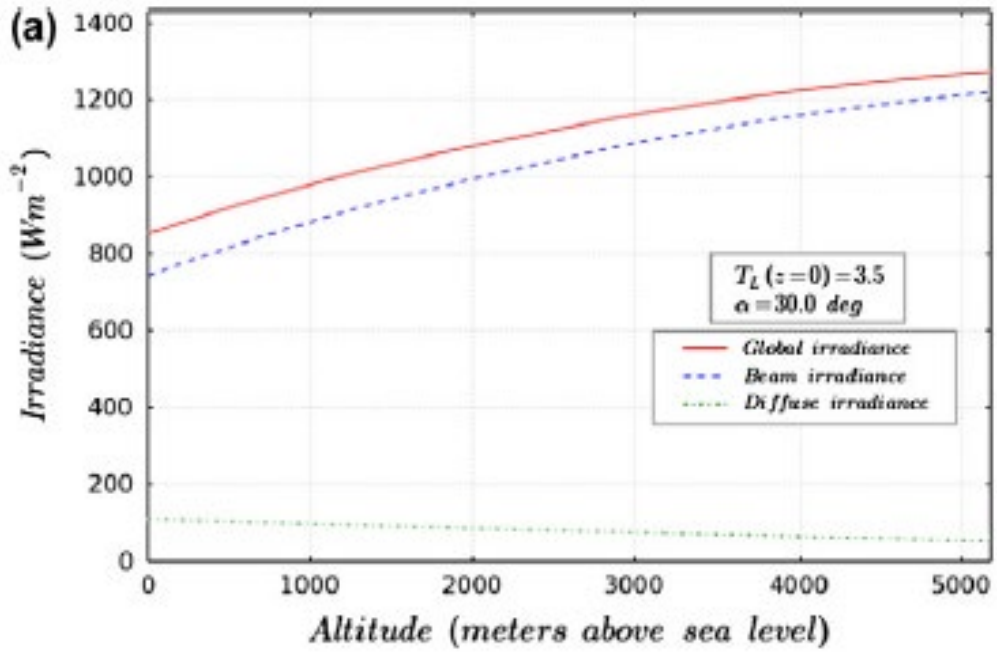

Figure 2.3 Vertical profile of global irradiance and its components according to the ESRA clear-sky model for Linke turbidity of 3.5 at sea level and solar altitude 30° [*Ruiz-Arias et al.*, 2010b].

$$R_{ah} = \frac{12}{\pi} G_{sc}\, d_r\, [(\omega_2 - \omega_1)\sin(\varphi)\sin(\delta) + \cos(\varphi)\cos(\delta)\,(\sin(\omega_2)\text{-}\sin(\omega_1))] \quad (2.30)$$

where G_{sc} is the solar constant [4.92 MJ m^{-2} h^{-1}], v_1 is the solar time at the beginning of the hour [radians] and v_2 is the solar time at the end of the hour [radians]. However, because this K_t depends on the solar zenith angle *Perez et al.* [1990] formulated a zenith angle-independent clearness index K_t' as

$$K_t' = \frac{K_t}{\left[1.031\exp\left(-\frac{1.4}{\left(0.9+\frac{9.4}{m}\right)}\right)+0.1\right]} \quad (2.31)$$

where m is the relative path length of the optical air mass [-]. Since the hourly zenith angle and m change considerably from hour to hour, this study follows *Perez et al.* [1990] who successfully used this approach in mountainous areas of southern Spain at the same latitude as northern New Mexico.

For beam radiation the effects of the relative length of air mass *m* [fraction] and the transmissivity of the sky τ [fraction] can be combined as

$$R_n = R_{ah}\,\tau^m \tag{2.32}$$

where τ is the atmospheric transmissivity (assumed constant at 0.6).

For calculation of the relative path length of an optical air mass at any elevation *z*, the relative path length of the optical air mass at sea level m_o is corrected for the atmospheric pressure at elevation *z* [*Iqbal*, 1983]

$$m_z = m_o \frac{P_z}{P_o} = m_o \frac{P}{101.3} \tag{2.33}$$

where P is calculated using Eq. (2.3) and m_o as

$$m_o = \sqrt{(1229 + (614\ cos\theta_{hor})^2)} - 614\ cos\theta_{hor} \tag{2.34}$$

Where $cos\theta_{hor}$ is the solar incidence angle on a horizontal surface.

The atmospheric pressures at the NLDAS and DEM pixels are calculated using Eq. (2.3) and named P_{NLDAS} and P_{DEM} [kPa], respectively. The relative effect of elevation on atmospheric attenuation of global radiation between z_{DEM} (the DEM resolution elevation) and the z_{NLDAS} (NLDAS resolution elevation) can then be calculated with Eq. (2.32) at both the NLDAS and the DEM elevations adjusting for the relative path length at each elevation using Eqs. (2.33) and (2.34). The relative optical path length correction (m_{pth}) from z_{NLDAS} to z_{DEM} is then calculated using the ratio between the relative optical path length at the NLDAS and DEM elevations:

$$m_{pth} = \frac{\tau^{m_{z,DEM}}}{\tau^{m_{z,NLDAS}}} \tag{2.35}$$

Gridded data of global horizontal hourly solar radiation from the NLDAS elevation (z_{NLDAS}) is then adjusted to global horizontal hourly solar radiation at the DEM elevation (z_{DEM}) incorporating relative pressure differences and optical path length using m_{pth}:

$$R_{sh}{}^{z_{DEM}} = R_{sh}{}^{z_{NLDAS}} * m_{pth} \tag{2.36}$$

2.2.1.2 Global Radiation Partitioning in Beam, Diffuse and Reflected Component

For the estimation of global radiation received on non-horizontal pixels the global horizontal hourly solar radiation at the DEM elevation (z_{DEM}) must be partitioned into its beam and diffusive components because the topographic effects for each of these is different and need to

be modeled separately [*Iqbal*, 1980]. The typical approach is to first estimate the diffuse radiation from the global radiation and then to calculate the beam radiation as the difference between the global radiation minus the diffuse radiation [e.g., *Liu and Jordan*, 1960]. *Ruiz-Arias et al.* [2010a] developed a statistical regression model for the determination of the diffuse fraction k_d that represents the diffuse radiation over the global radiation as a function of the clearness index K_t as defined in Eq. (2.29) as

$$k_d = 0.952 - 1.041\, e^{-\exp(2.300 - 4.702\, K_t)} \tag{2.37}$$

Thus, the diffuse solar radiation on a horizontal surface ${R_{sd}}^{z_{DEM}}$ can be calculated as

$${R_{sd}}^{z_{DEM}} = k_d \times {R_{sh}}^{z_{DEM}} \tag{2.38}$$

and the solar beam radiation on a horizontal surface ${R_b}^{z_{DEM}}$ as

$${R_b}^{z_{DEM}} = {R_{sh}}^{z_{DEM}} - {R_{sd}}^{z_{DEM}} \tag{2.39}$$

2.2.1.2.1 Beam Radiation on Tilted Pixel

The hourly beam radiation on a pixel with slope b and orientation or aspect g ($R_{b,\,bg}$ [MJ m^{-2} h^{-1}]) for a certain hour angel v is a function of the hourly beam radiation on a horizontal surface R_b, the zenith angle on a horizontal surface θ_z and a new corrected zenith angle for the sloping surface θ as [*Iqbal*, 1983]

$$R_{b,\beta\gamma} = R_b \left(\frac{cos\theta}{cos\theta_z}\right) \tag{2.40}$$

and

$$\cos\theta = \sin(\delta)\sin(\phi)\cos(\beta) - \sin(\delta)\cos(\phi)\sin(\beta)\cos(\gamma) + \cos(\delta)\cos(\omega)\cos(\phi)\cos(\beta) + \cos(\delta)\cos(\omega)\sin(\phi)\sin(\beta)\cos(\gamma) + \cos(\delta)\sin(\beta)\sin(\gamma)\sin(\omega) \tag{2.41}$$

where $\cos\theta$ is the cosine of the solar incident angle [radians] for sloped land surfaces, δ is the solar declination (positive in summer in the northern hemisphere) [radians], ϕ is the latitude of the pixel (positive for northern hemisphere) [radians], b is the slope [radians], where "b = 0" for a horizontal surface and "b = π/2" for a vertical surface (b is always positive and represents a upward/downward slope in any direction), γ is the surface aspect angle [radians], where "γ = 0" for surfaces facing south, γ is negative for east and positive for western aspect, "γ = -π/2" represents an east facing slope and "γ = +π/2" represents a west facing slope. "γ = -π" or "γ =π"

represents a north facing slope, and ω is the hour angle [radians]. The value of ω is equal to 0 at solar noon, ω is negative in the morning and positive in the afternoon.

The pixel receives direct sunlight if there is no self-shading due to its own slope or shading cast by its surrounding terrain. Self-shading occurs if the vector normal to its surface forms an angle greater than 90 degree (π/2 rad) with the solar vector. Shading occurs if the sun is hidden by a local horizon. Whether this happens is determined by comparing the illumination angle of the solar beam radiation with the horizon angle H in the direction of the sun. If the illumination angle is greater than the horizon angle shading will occur. The illumination angle is zero if the Sun is precisely overhead and 90 degrees at sunset and at sunrise. The horizon angle *H* is shown in Figure 2.4; the horizon angle in direction f is H_f. In this study the horizon angle was calculated for every hour with daylight in 36 directions over a forward distance of 50 km. A pixel in shade receives only diffuse radiation.

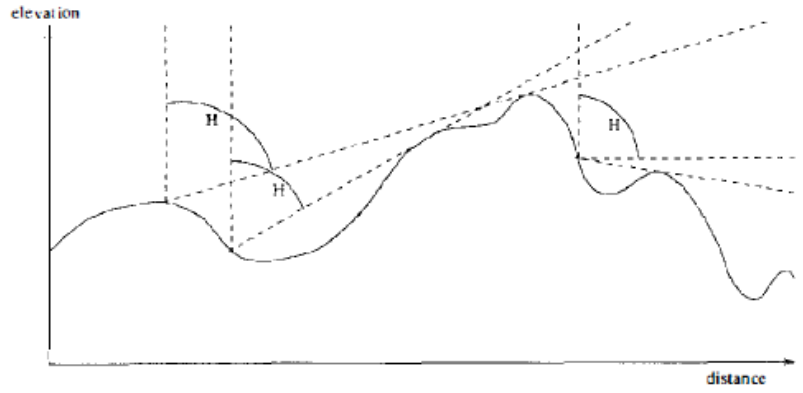

Figure 2.4. A single horizon profile showing the horizon angle *H* in the forward direction for three points [*Dozier and Frew*, 1990].

2.2.1.2.2 Diffuse Radiation on Tilted Pixel

The diffuse radiation on a pixel depends on the portion of the overlying hemisphere from which it receives diffuse radiation. On a pixel with slope b and orientation or aspect g the $R_{d,\,bg}$ [MJ m^{-2} h^{-1}]) is

$$R_{d,\beta\gamma} = R_d \times SVF \tag{2.42}$$

with the sky view factor *SVF* being the ratio between the diffuse component on the pixel and that on a horizontal unobstructed surface. Making the reasonable assumption that the diffuse radiation has an isotropic distribution over the hemispherical sky the SVF has a constant value

that can be expressed analytically in terms of the different horizons in each direction considered [*Dozier and Frew*, 1990]. For example, for eight directions f

$$SVF = \sum_{\phi=1}^{8} \cos(\beta)\, sin^2\left(H_\phi\right) + [\sin(\beta)\cos(\gamma)\left(H_\phi - sin\left(H_\phi\right)cos\left(H_\phi\right)\right)] \qquad (2.43)$$

2.2.1.2.3 Reflected Radiation on Tilted Pixel

The reflected radiation on a tilted pixel from surrounding terrain $R_{r,\,bg}$ [MJ m^{-2} h^{-1}]) can be calculated as

$$R_{r,\beta\gamma} = \alpha\left[\left(1 + \frac{\cos(\beta)}{2}\right) - SVF\right] \times (R_b + R_d) \qquad (2.44)$$

The hourly global radiation at each pixel is then calculated as

$$R_{g,\beta\gamma} = R_{b,\beta\gamma} + R_{d,\beta\gamma} + R_{r,\beta\gamma} \qquad (2.45)$$

2.2.2 Downscaling of Meteorological Data

Meteorological data is downscaled from the UofI METDATA gridded weather dataset [*Abatzoglou*, 2013]. The procedures used for downscaling follow the same methods applied by *Cosgrove et al.* [2003] in downscaling 40 km grid-cell meteorological data from the operational mesocale Eta numerical weather prediction model to the 1/8° (~12.5 x 12.5 km) NLDAS grid for NLDAS data. To calculate a Penman-Monteith Reference ET at the DEM scale, 1/24° (~4 x 4 km) UofI METDATA gridded min and max air temperature, specific humidity, and wind speed are resampled and adjusted to the 250 x 250 m ETRM grid cell size.

Min and max air temperature are lapsed based on elevation differences between UofI METDATA elevation and DEM resolution elevation. Wind speed is corrected from the 10 m measurement height of the data to the standard wind measurement height of 2 m for reference ET calculations. Atmospheric pressure is adjusted to the DEM resolution based on elevation. Specific humidity is adjusted keeping a constant relative humidity within each 4 km x 4km UofI METDATA grid-cell and specific humidity is calculated based on the lapsed temperature and elevation adjusted atmospheric pressure.

2.2.2.1 Downscaling of Air Temperature

Temperature differences between UofI METDATA and DEM grid cell elevations are calculated using the environmental lapse rate [*Cosgrove et al.*, 2003; *Shuttleworth*, 2012] for a standard atmosphere. Air temperature lapse rates vary strongly with season and depend on radiation and meteorological conditions [*Shuttleworth*, 2012]. Without a distributed calibrated lapse rate with time of year for an area encompassing the state of New Mexico, an average lapse rate must be

chosen to adjust air temperature with elevation. Lapse rates under most atmospheric conditions generally fall between a typical moist adiabatic lapse rate of 5 °C km^{-1} and a dry adiabatic lapse of 10 °C km^{-1}. When area specific lapse rates are not available, long-term records show that an average environmental lapse-rate of 6.5 °C km^{-1} fits temperature elevation data best within the lower atmosphere for the US as defined in the standard US Atmosphere [*Shuttleworth*, 2012].

Based on elevation differences between the UofI METDATA grid elevation (ZMET) and DEM grid elevation (ZDEM), T_{min} and T_{max} data is adjusted using the environmental lapse rate

$$T(Z)_{min} = T_{min} - \Gamma \times Z_{dif} \tag{2.46}$$

$$T(Z)_{max} = T_{max} - \Gamma \times Z_{dif} \tag{2.47}$$

Where Γ is the environmental lapse rate [6.5 °C km^{-1}], and Zdif = ZDEM – ZMET [m].

2.2.2.2 Elevation adjustment of Atmospheric Pressure

For a standard US atmosphere the atmospheric pressure can be determined through approximating the ideal gas law assuming hydrostatic pressure and standard temperature, using the approximation given by ASCE [2005] in Eq. (2.3). However, an improved approximation can be determined using hourly NLDAS pressure and temperature data at the NLDAS grid cell and the calculated average lapsed temperature estimated from the mean of the DEM lapsed min and max daily temperature. The NLDAS reference grid pressure can then be adjusted based on the temperature difference between the UofI METDATA mean daily air temperature and the lapsed daily air temperature

$$P(z) = P_0 \frac{(T_{mean} - \Gamma(z))}{T_{mean}}^{g/R*\Gamma} \tag{2.48}$$

Where T_{mean} is the average of the lapsed min and max temperature and R is the specific gas constant for dry air [8.314 J mol-1 K-1]. However, UofI METDATA does not include atmospheric pressure data and due to the difference of NLDAS data having only hourly timesteps and the daily time-steps for UofI METDATA, the pressure formula from ASCE [2005] in Eq. (2.3) is currently used to determine elevation adjusted atmospheric pressure from a reference sea-level pressure and temperature.

2.2.2.3 Downscaling of Specific Humidity

After calculating the lapsed average temperature and elevation adjusted pressure at the DEM grid scale, specific humidity is then subsequently adjusted with the equations given for reference ET calculations in flatlands in section 2.1. Following *Cosgrove et al.* [2003], relative humidity is held constant with elevation within the DEM grid cells contained in each UofI METDATA grid

cell. To calculate the adjusted specific humidity for the DEM grid cell the relative humidity of the UofI METDATA grid cell is determined from the actual and saturated vapor pressure using Eqs. (2.10) and (2.7) respectively. The saturated vapor pressure at the DEM grid cell is calculated using the lapsed average temperature. The ratio of actual and saturated vapor pressure for lapsed DEM values and UofI METDATA grid cell data are set equal to each other and the corrected DEM actual vapor pressure is calculated

$$e_a^{DEM} = e_s^{DEM} \frac{e_a^{MET}}{e_s^{MET}} \tag{2.49}$$

Where e_a^{MET} and e_a^{DEM} is the UofI METDATA and downscaled DEM actual vapor pressure respectively, e_s^{MET} and e_s^{DEM} is the UofI METDATA and the downscaled DEM saturated vapor pressure respectively.

2.2.2.4 Downscaling of Wind Speed

Wind speed data from UofI METDATA is given at a measurement height of 10 m (u_{10}) [m s^{-1}]. However, reference ET is calculated assuming air, temperature, humidity and wind speed data at a reference height of 1.5 – 2.5 m above the land surface [*ASCE-EWRI*, 2005] and therefore needs to be adjusted. Using the full logarithmic wind speed profile the wind speed is adjusted from 10 m (u_{10}) to 2 m (u_2):

$$\overline{u}_2 = \overline{u}_z \frac{4.87}{ln(67.8z_w - 5.42)} \tag{2.50}$$

No further modifications are done to the wind speed values between the UofI METDATA and the downscaled DEM wind speed values.

2.2.3 Downscaled Topography-Adjusted Reference ETr

The final step is to sum the hourly global radiation values calculated with Eq. (2.45) to the daily global radiation R_{g24}. This value and the downscaled meteorological data are used for the calculation of the daily topography adjusted reference ETr following the scheme depicted in Figure 2.2.

3. SOIL WATER BALANCE MODEL FOR ET ASSESSMENT USING THE CROP COEFFICIENT METHOD

One proven approach for the evaluation of ET from semi-arid partially vegetated lands is a simple soil water balance model [e.g., *Allen et al.*, 1998; *Jensen and Allen*, 2016; *Ritchie*, 1972]. Because this approach also yields an estimate of the groundwater recharge flux [*Daniel B. Stephens & Associates*, 2010; *Sandia National Laboratory*, 2007] it was selected for the evaluation of evapotranspiration and groundwater recharge over the entire state of New Mexico using the newly developed model Evapotranspiration and Recharge Model (ETRM) by *Ketchum et al.* [2016] and *Ketchum* [2016]. The purpose of this section is to present a description of the equations used in ETRM for assessment of daily evapotranspiration. The equations are taken from different key references [*Allen*, 2011; *Allen et al.*, 1998; *Allen et al.*, 2005a; *Allen et al.*, 2005b] but mostly follow the notation by [*Jensen and Allen*, 2016]. The model deals with partially or completely vegetated pixels that receive precipitation. Their actual evapotranspiration ($ET_{c\ act}$) on day *i* (mm/day) is

$$ET_{c\ act,i} = K_{c\ act,i} ET_{r,i} = (K_{s,i} K_{cbr,i} + K_{er,i}) ET_{r,i} \tag{3.1}$$

where on day *i* the $K_{c\ act,i}$ is the "actual" crop coefficient that includes the effect of environmental stresses; $ET_{r,i}$ is the reference ET for a tall crop (mm/day); $K_{s,i}$ is a dimensionless transpiration reduction coefficient [0.0 - 1.0] that reduces $K_{cbr,i}$ when the average soil water content in the root zone cannot sustain full plant transpiration; $K_{cbr,i}$ is the basal crop coefficient that represents the ratio of ET_c/ET_r under conditions when the soil surface layer is dry, but where the average soil water content of the root zone is adequate to sustain full plant transpiration; $K_{er,i}$ is the soil evaporation coefficient that represents the majority of evaporation from soil following wetting by precipitation or irrigation. The calculation of the tall crop reference $ET_{r,i}$ is discussed in Section 3. Our challenge is to determine $ET_{c\ act,i}$ for each pixel within New Mexico on each day of the time period 2000 through 2013.

The basal crop coefficient $K_{cbr,i}$ is estimated as [Appendix G in *Jensen and Allen*, 2016; *Rafn et al.*, 2008]

$$K_{cbr,i} \approx 1.25\ NDVI_i \tag{3.2}$$

where $NDVI_i$ is the Normalized Difference Vegetation Index obtained from the MOD13Q1 product at a spatial resolution of 250×250 m that consists of the NDVI observed by MODIS for each 16 day period of the year. We obtain the daily $NDVI_i$ by linear interpolation between the center days of two consecutive 16 day periods (Fig. 2). Eq. (3.2) produces good results in agricultural areas [*Allen et al.*, 2011] but will be evaluated for native vegetation and adapted –if needed– in our project. The use of a vegetation coefficient for determination of a crop coefficient is a common procedure for evaluation of ET on a regional scale [*Nagler et al.*, 2005].

The stress coefficient $K_{s,i}$ is determined as

$$K_{s,i} = \frac{TAW - D_{r,i-1}}{TAW - RAW} = \frac{TAW - D_{r,i-1}}{(1-p)TAW} \qquad for\ D_{r,i-1} > RAW \tag{3.3}$$

where *TAW* is the total available water (mm) that can be stored in the root zone of the vegetation, *RAW* is readily available water in the root zone (mm), $D_{r,i}$ is the depletion of the root zone (mm), and *p* is the fraction of *TAW* that can be depleted before water stress and ET reduction occur (Fig. 3). Parameter p varies from 0.3 for shallow rooted plants at high rates of $ET_{c\ act}$ (>8.0 mm/day) to 0.7 for deep rooted plants at low rates of $ET_{c\ act}$ (<3.0 mm/day). When $D_{r,i} \leq RAW$ then K_s=1.0. The total available water (*TAW*) that can be stored in the root zone is

$$TAW = (WCFC - WCWP)Z_r \tag{3.4}$$

where *WCFC* is the soil water content at field capacity (m^3/m^3), *WCWP* is the soil water content at wilting point (m^3/m^3), and Z_r is the effective rooting depth (mm) that contains the effective depth of the evaporation layer Z_e (mm). Values for WCFC and WCWP are derived from a soil data base using pedotransfer functions while Z_r is estimated from the USGS 2010 land cover map.

The soil water balance for the root zone in terms of depletion is

$$D_{r,i} = D_{r,i-1} - (P_i - RO_i) - I_i - CR_i + ET_{c\ act,i} + DP_i \tag{3.5}$$

where on each day *i* P_i is precipitation (mm/day), RO_i is runoff from the soil surface but in steep terrain this term also includes interflow (mm/day), I_i is net irrigation depth that infiltrates the soil (mm/day), CR_i is the capillary rise from the groundwater table (mm/day) and DP_i is water loss out of the root zone by deep percolation (mm/day). The focus on our current study is to obtain estimates of $ET_{c\ act,i}$ that respect the water balance for relatively flat desert areas. Therefore, for now the terms RO_i, I_i, and CR_i are considered zero and Eq. (3.5) becomes

$$D_{r,i} = D_{r,i-1} - P_i + ET_{c\ act,i} + DP_i \tag{3.6}$$

The limits imposed on $D_{r,i}$ are

$$0 \leq D_{r,i} \leq TAW \tag{3.7}$$

but the lower limit of zero can be relaxed if some delayed drainage from the root zone is allowed as discussed below with Eq. (3.9).

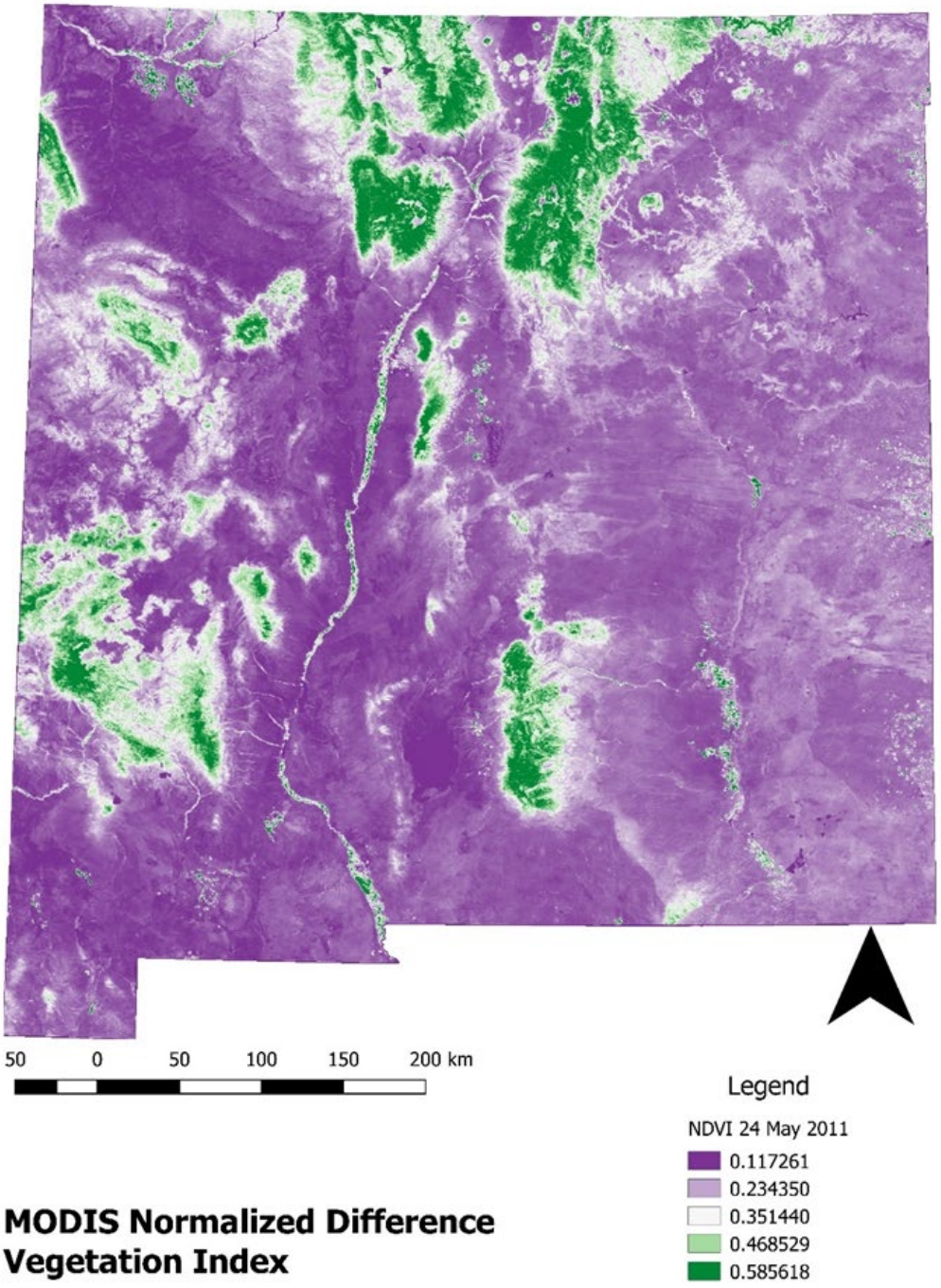

Figure 3.1 The MODIS Normalized Difference Vegetation Index (NDVI) on 24 May 2011 [*Ketchum et al.*, 2016]. The NDVI is the ratio of the difference between the spectral reflectance of the near-infrared and visible red bands over the sum of these two reflectances. Its value varies between 0 and 1 for land surfaces but becomes negative for water bodies.

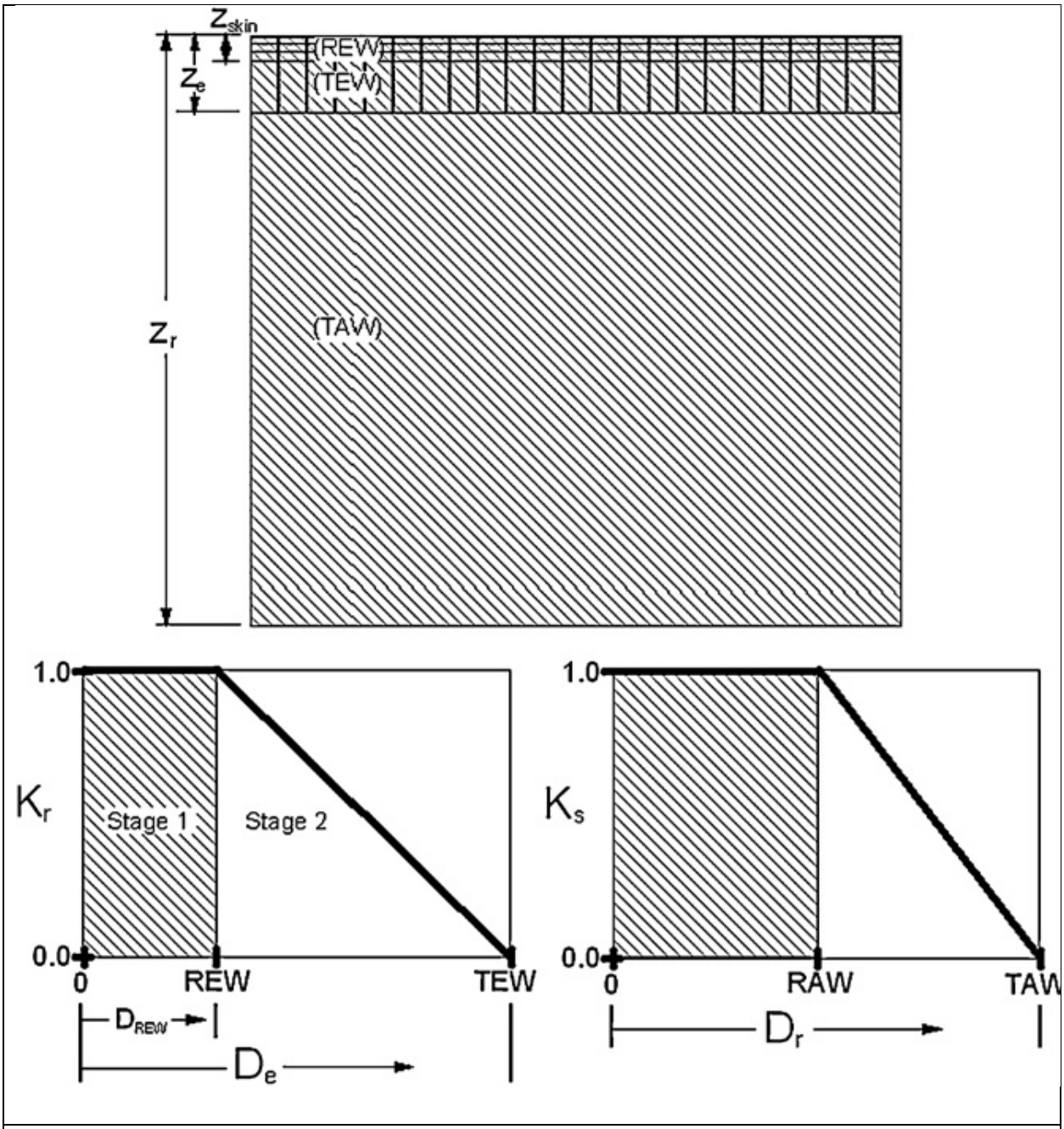

Figure 3.2 Schematic showing a soil profile (top) where the 'skin' layer, z_{skin}, the evaporation layer, z_e, and rooting depth, z_r , are marked. Maximum evaporable or extractable depths of water in each layer are also shown, where REW is associated with z_{skin}, TEW is associated with z_e, and TAW is associated with z_r . Depths z_{skin} and z_e are subsets of (and therefore included in) z_r . Water depths REW and TEW are subsets of (and therefore included in) TAW. REW is a subset of, and is included in, TEW; also shown are the K_r vs. D_e function (bottom left) and the K_s vs. D_r function (bottom right) that are used to reduce evaporation rate or basal ET rate as soil dries. Figure and caption by *Allen* [2011].

Deep percolation DP_i can only occur when heavy rainfall increases soil water content in the root zone above field capacity, i.e. above *TAW*, so that the depletion $D_{r,i}$ becomes zero and

$$DP_i = P_i - ET_{c\ act,i} - D_{r,i-1} \tag{3.8}$$

where DP_i is limited to $DP_i \geq 0$. Since under this condition $D_{r,i} < RAW$ the stress factor K_s = 1.0 and $ET_{c\ act,i} = (K_{cb,i} + K_{e,i})ET_{r,i}$. As long as soil water content in the root zone is below field capacity, i.e below *TAW*, the depletion $D_{r,i} > 0$ and the soil is assumed not to drain and DP_i = 0. If drainage from the root zone is expected to be delayed following a large infiltration event or due to a low conductivity of the bedrock, then DP_i is estimated as

$$DP_i = \max(\min\left[(P_i - ET_{c\ act,i} - D_{r,i-1})\ ,\ K_{sat\ bedrock}\right], 0) \tag{3.9}$$

assuming unit gradient conditions at the interface between bedrock with saturated hydraulic conductivity $K_{sat\ bedrock}$ and bottom of the root zone. Limiting DP_i to $K_{sat\ bedrock}$ has the effect of causing $D_{r,i}$ in Eq. (3.6) to be negative for one or more days.

$K_{c\ max\ r}$ is the maximum value of $K_{c\ act}$ following rain or irrigation and represents an upper limit on evaporation and transpiration from the vegetated surface. It is a measure of the natural constrains on available energy. For the tall reference ET_r

$$K_{c\ max\ r} = \max[1.0, (K_{cbr} + 0.05)] \tag{3.10}$$

A general model for the soil evaporation coefficient K_{er} for estimating the evaporation from the surface layer of soil after rain or irrigation for use with the basal crop coefficient K_{cbr} is

$$K_{er,i} = K_{r,i}\left(K_{c\max r,i} - K_{s,i}K_{cbr,i}\right) \qquad such\ that\ K_{er,i} \leq f_{ew,i}K_{c\max r,i} \tag{3.11}$$

where $K_{r,i}$ is a dimensionless evaporation reduction coefficient. In Eq. (3.11) transpiration is given priority access to the available energy over evaporation because $K_{s,i}K_{cbr,i}$ is subtracted from $K_{c\max r,i}$ before calculation of $K_{er,i}$. For a completely bare soil $K_{s,i}K_{cbr,i}$ is set equal to zero. The parameter f_{ew} is the fraction of soil surface from which most of the evaporation occurs and is generally taken as the fraction of the soil surface that is both exposed to drying and is "wetted" during the wetting event. The parameter f_w is the average fraction of soil surface wetted by precipitation or irrigation. For precipitation f_w=1 and

$$few = 1 - fc \tag{3.12}$$

where parameter f_c is the fraction of ground surface coverage by vegetation. Both (1 - f_c) and f_w, for numerical stability, have limits of [0.01 - 1].

For purposes of estimating f_{ew}, f_c can be estimated using a general relationship between f_c and K_{cb} from FAO-56 as

$$f_{c,i} = \left(\frac{K_{cbr,i} - K_{c\,min}}{K_{c\max r,i} - K_{c\,min}}\right)^{1+0.5h} \quad (3.13)$$

where $K_{c\,min}$ is the minimum (basal) K_c for dry bare soil with no ground cover and h is the height of the crop in m. The differences between $K_{cbr,i} - K_{c\,min}$ and $K_{c\max r,i} - K_{c\,min}$ are limited to ≥ 0.01 for numerical stability. The value for f_c will change daily as $K_{cbr,i}$ changes.

$K_{c\,min}$ ordinarily has the same value as the $K_{cbr,i}$ during the initial growth period for annual crops, $K_{cb\,ini}$, that represents nearly bare soil conditions (i.e., $K_{c\,min} \sim 0.10$ to 0.15). However, $K_{c\,min}$ is set to 0 or nearly zero under conditions having large time periods between wetting events, for example in applications with natural vegetation in deserts. The value for $f_{c,i}$ decreases during the late season period in proportion to $K_{cbr,i}$ to account for local transport of sensible heat from senescing leaves to the soil surface.

A common model for soil evaporation considers two stages of evaporation: the energy limiting stage 1, and the falling stage 2. When the soil is wet (in stage 1) the evaporation reduction factor $K_{r,i}$ is assumed to be 1.0. When the water content in the effective evaporation layer begins to limit evaporation (in stage 2), $K_{r,i}$ decreases below 1.0. The value for $K_{r,I}$ is set to zero when the total amount of water in the effective evaporation layer is depleted during the drying cycle. The depth of the evaporation layer tends to be between 0.1 and 0.15 m. Assuming that the soil in the evaporation layer is at field capacity (WCFC) shortly after rainfall or irrigation and that it can dry to halfway between 0 and the wiltingpoint (WCWP), the total amount of water that can be depleted by evaporation (TEW) from the effective evaporation layer during one drying cycle is estimated as:

$$TEW = (WCFC - 0.5\,WCWP)Z_e \quad (3.14)$$

Where *TEW* is the total evaporable water (mm) and Z_e is the effective depth of the evaporation layer (mm). The cumulative depth of evaporation or depletion D_e at the end of stage 1 is the readily evaporable water (*REW*) that normally ranges from 5 to 12 mm depending on soil texture.

During winter or other cool periods, less radiation energy is available for heating the soil surface layer and evaporate water so that total effective *TEW* during a drying event will typically be smaller than during a warm period. Therefore, *Allen et al.* [1998] suggested taking reference ET_r as a surrogate for temperature and radiation conditions to reduce the value of *TEW*. When $ET_r < 4$ mm/day, *TEW* is estimated as

$$TEW = (WCFC - 0.5\,WCWP)Z_e\sqrt{\frac{ET_r}{4}} \quad (3.15)$$

where ET_r is an average representing the general estimation period in mm/day. A monthly average for ET_r is recommended because varying ET_r on a daily basis is not recommended since it will cause *TEW* to vary daily, which can cause numerical inconsistencies.

During the falling rate stage 2, where D_e > REW, the evaporation rate is estimated in proportion to the amount of water remaining in the evaporation layer, and $K_{r,i}$ is calculated as

$$K_{r,i} = F_{stage1} + \left(1 - F_{stage1}\right)\max[\min\left(\frac{TEW - D_{e,i-1}}{TEW - REW}, 1.0\right), 0.0] \quad (3.16)$$

where $D_{e,\,i-1}$ is the cumulative depth of evaporation at the end of timestep (i-1), representing the previous timestep, and F_{stage1} is the fraction of the time step (day or hour) that resides in stage 1 evaporation. 1 – F_{stage1} of the time step resides in stage 2. This formulation can be important when using daily calculation timesteps, especially for coarse soils having small *REW*.

The fraction of calculation timestep i that resides in stage 1, F_{stage1}, is not approximated using a time scale but rather

$$F_{stage1} = \frac{REW - D_{REW_{i-1}}}{K_{c\max r,i}\ ET_{r,i}} \qquad , 0 \le F_{stage1} \le 1.0 \quad (3.17)$$

where where $D_{REW,\,i-1}$ is the the depletion of the upper "skin" soil surface layer that directly contributes to stage 1 drying, mm, at the end of timestep i-1, and $K_{c\max r,i}$ is the value for K_e expected during stage 1 drying. The value for $K_{e\,max}$ (=$K_{c\max r,i}$) is tied to the reference ET type, where $K_{e\,max}$ ~ 1.0 is recommended when using the alfalfa reference, ET_r. The water balance equation for determining $D_{REW_{i-1}}$ is given later as Eq. (3.22).

The evaporation E_i on day i is calculated as

$$E_i = K_{er,i} ET_{r,i} \qquad where\ K_{er,i} \le K_{c\max r,i} \quad (3.18)$$

Estimation of $K_{er,i}$ using the FAO evaporation model via Eq. (3.11) requires a water balance conducted for the f_{ew} fraction of the surface soil layer on a daily or shorter timestep

$$D_{e,i} = D_{e,i-1} - \left[(1 - f_b)(P_i - RO_i + \frac{I_i}{f_w}\right) + f_b(P_{i+1} - RO_{i+1} + \frac{I_{i+1}}{f_w})\Big] + \frac{E_i}{f_{ew}} + T_{e,i} \quad (3.19)$$

where $D_{e,i-1}$ and $D_{e,i}$ are cumulative depletion depth at the ends of days i-1 and i [mm], P_i and RO_i are precipitation and precipitation runoff from the soil surface on day i [mm], I_i is the irrigation depth on day i that infiltrates the soil [mm], E_i is evaporation on day i (i.e., $E_i = K_{er,i}$ $ET_{r,i}$) [mm], $T_{e,\,i}$ is the depth of transpiration from the exposed and wetted fraction of the soil surface layer on day i [mm], and f_b is the fraction of the precipitation and irrigation during a calculation time step (hour or day) that is assumed to contribute immediately to evaporation during that same timestep, with 1 - f_b of the precipitation and irrigation not contributing to evaporation until the following timestep, on average. If unknown, f_b can be set to 0.5. f_b has limits of 0 and 1.0. f_b effectively controls the immediacy of evaporation from a wetting event that may occur at an unknown time within the calculation timestep, for example, nighttime irrigations during a daily timestep. Eq. (3.19) is a form for $D_{e,i}$ proposed by *Allen* [2011] to distribute P and I between adjacent timesteps in regard to their influence on the timing of the

increase in E stemming from the wetting event. This may be important for daily timesteps, but generally is not important for hourly or shorter timesteps. Variables having subscripts 'i+1' indicate values for the timestep following current timestep i. Assuming that the surface layer is at field capacity following heavy rain or irrigation, the minimum value for $D_{e,i}$ is zero. The deep percolation term of the original FAO-56 formulation for Eq. (3.19) is omitted in the new equation forms for Eqs. (3.19) and (3.20), as it is not needed. Instead, $D_{e,i}$ and $D_{e,i-1}$ are constrained to limits of $0 \leq D_{e,i} \leq TEW$. Any P or I additions in excess of $D_{e,i}$ (and $D_{REW,i}$ in Eq.) are assumed to infiltrate to depths in the soil below Z_e (or below the skin in the case of $D_{REW,i}$).

For shallow rooted annual crops having rooting depth less than about 0.5 m, transpiration from the evaporative layer $T_{e,I}$ may have a significant effect on the water balance of the surface layer and therefore on *estimation* of the evaporation component during the development period.

For our prototype model RO_i, I_i and $T_{e,i}$ are not taken into account so that Eq. (3.19) reduces to

$$D_{e,i} = D_{e,i-1} - [(1 - f_b)P_i + f_b P_{i+1}] + \frac{E_i}{f_{ew}} \tag{3.20}$$

The parameter $D_{REW\,i-1}$ in Eq. (3.17) is the depletion of water from the *REW* layer, referred to as the skin layer, at the end of the prior i-1 timestep. Eq. (3.17) estimates the $F_{stage\,1}$ parameter used in Eq. (3.16) to simulate any stage 1 evaporation that may occur from light wetting events or from heavy wetting events. Background is given in *Allen* [2011]. For light wetting events, stage 1 evaporation may last for only part of a single timestep. The calculation of $D_{REW\,i}$ is designed, similar to Eq. (3.19), to be forward looking with regard to the wetting event to consider soil surface wetting and corresponding evaporation from a wetting event occurring during the current timestep i

$$D_{REW,i} = D_{REW,i-1} - \left[(1 - f_b)(P_i - RO_i + \frac{I_i}{f_w}\right) + f_b(P_{i+1} - RO_{i+1} + \frac{I_{i+1}}{f_w})\Big] + \frac{E_i}{f_{ew}} \tag{3.21}$$

where $D_{REW\,i-1}$ and $D_{REW\,i}$ are cumulative depletion depths at the ends of day i-1 and i (mm). Both terms are constrained to limits $0 \leq D_{REW,i} \leq REW$.

Again for our prototype model Eq. (3.21) becomes

$$D_{REW,i} = D_{REW,i-1} - [(1 - f_b)P_i + f_b P_{i+1}] + \frac{E_i}{f_{ew}} \tag{3.22}$$

4. RESULTS

Main study objective was to develop a procedure for the calculation of daily reference ETr at a spatial resolution adequate for assessment of evapotranspiration and groundwater recharge in the mountainous regions of New Mexico at a spatial resolution of 250 m. The procedure for calculation of the daily ETr over the entire state of New Mexico is described in Chapter 2 and the procedure for calculation of the daily evapotranspiration and groundwater recharge is described in Chapter 3 and with much greater detail in the report by *Ketchum et al.* [2016]. Figure 4.1 presents the daily reference ETr on March 24, 2008 (mm/day) calculated using the equations presented in Chapter 2 and Figures 2.1 and 2.2. Figure 4.2 shows the percentage of the total annual precipitation that leaves the soil as evapotranspiration. In the lower areas of the state all precipitation is lost by evapotranspiration while at higher elevations in the mountains less precipitation is lost by ET and, therefore, groundwater recharge can take place.

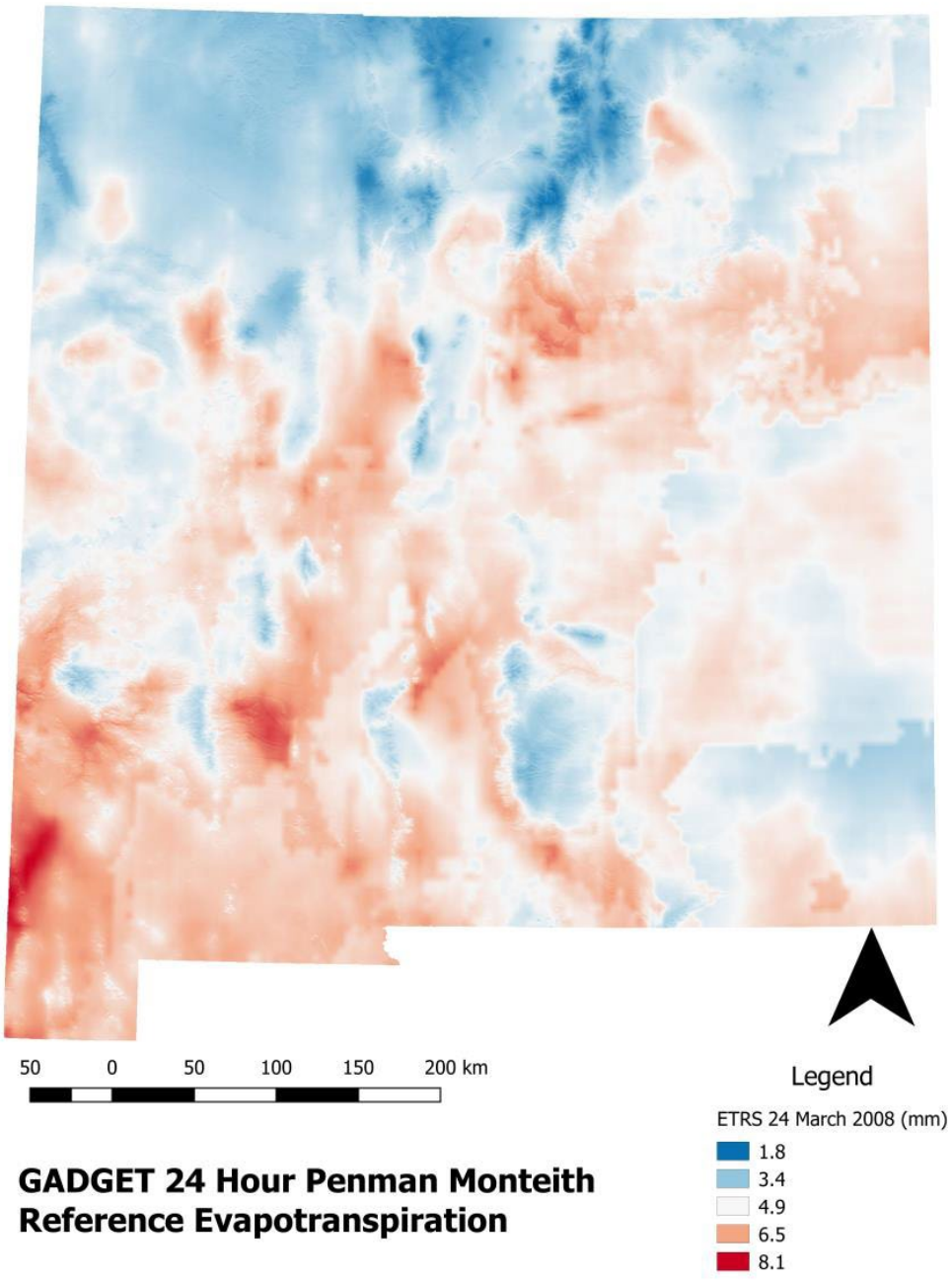

Figure 4.1 Gridded Atmospheric Data Downscaling Evapotranspiration Tools (GADGET) for High-Resolution Distributed Reference ET in Complex Terrain creates 250 m resolution gridded data representing tall-crop reference ET, the basis for energy-driven components of the ETRM. Red represents high reference ET [*Ketchum et al.*, 2016].

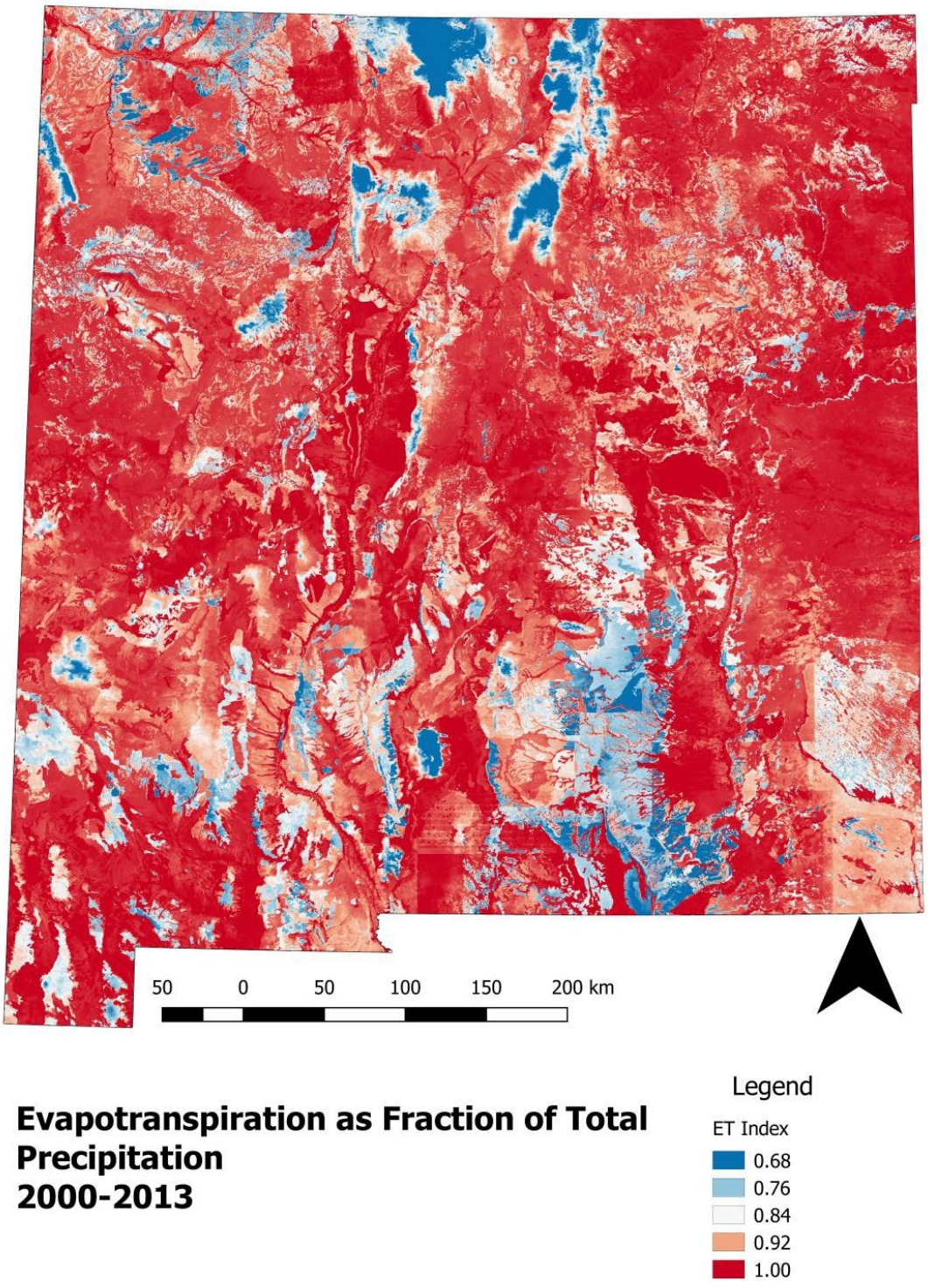

Figure 4.2 The ET Index (i.e., the fraction of precipitation lost to ET) shows ET is the dominant flux of water out of the soil layer. Over 85% of the state loses 70% of precipitation to evapotranspiration, by far the dominant flux of water from the soil layer [*Ketchum et al.*, 2016].

5. CONCLUSIONS AND RECOMMENDATIONS

We have successfully used existing information in the literature for the development of a procedure for the calculation of daily reference ETr at a spatial resolution adequate for assessment of evapotranspiration and groundwater recharge in the mountainous regions of New Mexico at a spatial resolution of 250 m. The procedure for calculation of the daily ETr takes the topography into account so that more accurate estimates of groundwater recharge can be obtained.

The first version of our algorithms produce reasonable results but future validations and sensitivity analyses are needed to improve the basic procedure reported in this study.

REFERENCES

Abatzoglou, J. T. (2013). Development of gridded surface meteorological data for ecological applications and modelling. *International Journal of Climatology*, *33*(1), 121–131. http://doi.org/10.1002/joc.3413

Abatzoglou, J. T. (2013), Development of gridded surface meteorological data for ecological applications and modelling, *International Journal of Climatology*, *33*(1), 121-131.

Aguilar, C., J. Herrero, and M. J. Polo (2010), Topographic effects on solar radiation distribution in mountainous watersheds and their influence on reference evapotranspiration estimates at watershed scale, *Hydrol. Earth Syst. Sci.*, *14*(12), 2479-2494.

Allen, R. G. (2011), Skin layer evaporation to account for small precipitation events—An enhancement to the FAO-56 evaporation model, *Agric. Water Manage.*, *99*(1), 8-18.

Allen, R. G., L. S. Pereira, D. Raes, and M. Smith (1998), *Crop evapotranspiration: Guidelines for computing crop requirements. Irrigation and Drainage Paper No. 56.*, 300 pp., Food and Agricultural Organization of the United Nations, Rome, Italy.

Allen, R. G., L. S. Pereira, M. Smith, D. Raes, and J. L. Wright (2005a), FAO-56 dual crop coefficient method for estimating evaporation from soil and application extensions, *Journal of Irrigation and Drainage Engineering*, *131*(1), 2-13.

Allen, R. G., W. O. Pruitt, D. Raes, M. Smith, and L. S. Pereira (2005b), Estimating evaporation from bare soil and the crop coefficient for the initial period using common soils information, *Journal of Irrigation and Drainage Engineering*, *131*(1), 14-23.

Allen, R. G., A. Irmak, R. Trezza, J. M. H. Hendrickx, W. G. M. Bastiaanssen, and J. Kjaersgaard (2011), Satellite-based ET estimation in agriculture using SEBAL and METRIC, *Hydrologic Processes*, *25*, 4011–4027.

ASCE-EWRI (2005), *The ASCE standardized reference evapotranspiration equation.*, 59 p. with six appendices pp., Environmental and Water Resources Institute, American Society of Civil Engineers, Reston, Virginia.

Barry, R. G. (2008), *Mountain weather and climage. Third edition.*, 506 pp., Cambridge University Press, New York.

Beven, K. (1979), A sensitivity analysis of the Penman-Monteith actual evapotranspiration estimates, *J. Hydrol.*, *44*(3-4), 169-190.

Cosgrove, B. A., et al. (2003), Real-time and retrospective forcing in the North American Land Data Assimilation System (NLDAS) project, *Journal of Geophyical Research*, *108(D22)*, 8842, doi:8810.1029/2002JD003118.

Daniel B. Stephens & Associates, I. (2010), Draft - Manual for the Distributed Parameter Watershed Model (DPWM)*Rep.*, 83 pp, Daniel B. Stephens & Associates, Inc., Albuquerque.

Dozier, J., and J. Frew (1990), Rapid calculation of terrain parameters for radiation modeling from digital elevation data, *Geoscience and Remote Sensing, IEEE Transactions on*, *28*(5), 963-969.

Gee, G. W., and D. Hillel (1988), Groundwater recharge in arid regions: review and critique of estimation methods, *Hydrol. Process.*, *2*, 255-266.

Hendrickx, J. M. H., and G. Walker (1997), Chapter 2 Recharge from precipitation, in *Recharge of phreatic aquifers in (semi)-arid areas*, edited by I. Simmers, pp. 19-114, Balkema, Rotterdam, The Netherlands.

Iqbal, M. (1980), Prediction of hourly diffuse radiation from measured hourly global radiation on a horizontal surface, *Sol. Energy*, *24*, 491-503.

Iqbal, M. (1983), *An introduction to solar radiation*, 390 pp., Academic Press, Toronto.

Jensen, M., and R. Allen (2016), *Evaporation, Evapotranspiration, and Irrigation Water Requirements. Second Edition. ASCE Manual and Report No. 70*, 554 pp., American Society of Civil Engineers.

Jensen, M. E., and R. G. Allen (Eds.) (2015), *Evaporation, Evapotranspiration and irrigation water requirements. Second Edition. ASCE Manual and Report No. 70*, 562 pp., American Society of Civil Engineers, Reston, Virginia.
Kearns, A. K., and J. M. H. Hendrickx (1998), *Temporal variability of diffuse groundwater recharge in New Mexico*, 43 pp., New Mexico Water Resources Research Institute, New Mexico State University, Las Cruces NM.
Ketchum, D. (2016), Evapotranspiration and recharge model (ETRM) for New Mexico, in progress pp, New Mexico Tech, Socorro NM.
Ketchum, D., B. T. Newton, and F. Phillips (2016), High-resolution estimation of groundwater recharge for the entire state of New Mexico using a soil water balance model*Rep.*, draft submitted pp, New Mexico Water Resources Research Institute, Las Cruces NM.
Leuning, R., Y. Q. Zhang, A. Rajaud, H. Cleugh, and K. Tu (2008), A simple surface conductance model to estimate regional evaporation using MODIS leaf area index and the Penman-Monteith equation, *Water Resour. Res.*, *44*(10), n/a-n/a.
Lewis, C. S., H. M. E. Geli, and C. M. U. Neale (2014), Comparison of the NLDAS Weather Forcing Model to Agrometeorological Measurements in the western United States, *J. Hydrol.*, *510*(0), 385-392.
Liu, B. Y. H., and R. C. Jordan (1960), The interrelationship and characteristic distribution of direct, diffuse and total solar radiation, *Solar Energy*, *4*(3), 1-19.
Monteith, J. L., and M. H. Unsworth (2008), *Principles of environmental physics. Third Ed.*, 418 pp., Academic Press, London, UK.
Nagler, P. L., J. Cleverly, E. Glenna, D. Lampkin, A. Huete, and Z. Wan (2005), Predicting riparian evapotranspiration from MODIS vegetation indices and meteorological data, *Remote Sensing of Environment*, *94*, 17-30.
Nitu, R., and K. Wong (2010), CIMO SURVEY ON NATIONNAL SUMMARIES OF METHODS AND INSTRUMENTS FOR SOLID PRECIPITATION MEASUREMENT AT AUTOMATIC WEATHER STATIONS. INSTRUMENTS AND OBSERVING METHODS REPORT No. 102*Rep.*, 57 pp, WORLD METEOROLOGICAL ORGANIZATION.
Perez, R., P. Ineichen, R. Seals, and A. Zelenka (1990), Making full use of the clearness index for parameterizing hourly insolation conditions, *Solar Energy*, *45*(2), 111-114.
Rafn, E., B. Contor, and D. Ames (2008), Evaluation of a Method for Estimating Irrigated Crop-Evapotranspiration Coefficients from Remotely Sensed Data in Idaho, *Journal of Irrigation and Drainage Engineering*, *134*(6), 722-729.
Ritchie, J. T. (1972), Model for predicting evaporation from a row crop with incomplete cover, *Water Resour. Res.*, *8*(5), 1204-1213.
Ruiz-Arias, J. A., H. Alsamamra, J. Tovar-Pescador, and D. Pozo-Vázquez (2010a), Proposal of a regressive model for the hourly diffuse solar radiation under all sky conditions, *Energy Conversion and Management*, *51*(5), 881-893.
Ruiz-Arias, J. A., T. Cebecauer, J. Tovar-Pescador, and M. Šúri (2010b), Spatial disaggregation of satellite-derived irradiance using a high-resolution digital elevation model, *Solar Energy*, *84*(9), 1644-1657.
Sandia National Laboratory (2007), Simulation of net infiltration for present-day and potential future climates, Yucca Mountain Project. MDL-NBS-HS-000023 REV 01. May 2007.*Rep.*
Schmugge, T. J., S. Walker, and J. M. H. Hendrickx (2016), Mapping statewide precipitation and evapotranspiration in New Mexico: Year One*Rep.*, draft submitted pp, New Mexico Water Resources Research Institute, Las Cruces, NM.
Senay, G. B., J. P. Verdin, R. Lietzow, and A. M. Melesse (2008), Global Daily Reference Evapotranspiration Modeling and Evaluation, *JAWRA Journal of the American Water Resources Association*, *44*(4), 969-979.

Shuttleworth, W. J. (2006), Towards one-step estimation of crop water requirement, *Transactions of the ASABE*, *49*(4), 925−935.
Shuttleworth, W. J. (2012), *Terrestrial Hydrometeorology*, 450 pp., John Wiley & Sons, Ltd West Sussex, UK.
Smith, M., R. Allen, J. Monteith, A. Perrier, L. Pereira, and A. Segeren (1991), Report of the expert consultation on procedures for revision of FAO guidelines for prediction of crop water requirements*Rep.*, 54 pp, UN-FAO, Rome, Italy.
Wallace, J. M., and P. V. Hobbs (2006), *Atmospheric science. An introductory survey. Second Edition*, 483 pp., Elsevier, Amsterdam.